SHORT-TERM FREEWAY TRAFFIC PREDICTION BY PAYNE-WHITHAM MODEL CONSIDERING DRIVER'S ANTICIPATION EFFECT

A Thesis

by

XIAOYU GUO

Submitted to the Office of Graduate and Professional Studies of
Texas A&M University
in partial fulfillment of the requirements for the degree of

MASTER OF SCIENCE

Chair of Committee,	Yunlong Zhang
Committee Members,	Xiubin Wang
	Prabir Daripa
Head of Department,	Robin Autenrieth

May 2019

Major Subject: Civil Engineering

ABSTRACT

In this research, we study a macroscopic traffic model, Payne-Whitham (PW) model, with an anticipation source term. The anticipation source describes how the traffic adjusts its speed based on the condition ahead. With the calibration of driver's anticipation effect in PW model, this study 1) proposes a short-term freeway traffic prediction method, 2) validates the method with real world data from PeMS, 3) assesses the method by MAPE, VAPE and PPE, 4) compares the method in different traffic conditions and prediction periods, 5) provides a guideline in the range of driver's anticipation parameter. The results indicate the average relative error of predicting speed in 5-min is 3.48% with a variance of 5.33%. The comparisons revealed the anticipation parameter increases with a decreasing in the size of predictable VDSs as the traffic becomes more congested. For a longer prediction period, the reduction in the size of predictable VDSs is higher. We recommend taking a value between 8 to 14 for the anticipation parameter when modelling the traffic with LOS from C to F; from 3 to 9 for traffic between LOS B and C; from 0 to 4 for traffic with LOS A. These recommended ranges could guide practitioners without knowing the shape of traveling wave when using PW model or PW prediction method. The traffic prediction method developed in this study differs from data-driven prediction methods. It is derived from the solutions of PW model; hence, it underlies flow studies and the process includes the concept of traffic dynamics. It reduces the size of predictable data points, because a perturbation method was assumed in solving the PW model. The results show under a congested traffic, there are about 77.6% of data points satisfied for a 5-min PW prediction, 63.6% of data points satisfied for a one-hour PW prediction. This indicates the limitation does not have large impact on the PW predictions in general.

ACKNOWLEDGEMENTS

I would like to thank my committee chair, Dr. Yunlong Zhang, and my committee members, Dr. Bruce Wang, Dr. Prabir Daripa, for their guidance and support throughout the course of this research. I also appreciate the help from Dr. Alireza Talebpour and Dr. Brian J. Spencer.

Thanks also go to my friends and colleagues and the department faculty and staff for making my time at Texas A&M University a great experience. Finally, thanks to my family for their encouragement, patience and love.

CONTRIBUTORS AND FUNDING SOURCES

Contributors

This work was supervised by a thesis committee consisting of Professors Yunlong Zhang and Xiubin Wang of the Zachry Department of Engineering and Professor Prabir Daripa of the Department of Mathematics.

The naive version of solving Payne-Whitham model in the methodology for Chapter 3 was completed by the student, under the supervision of Dr. Brian J. Spencer from the Department of Mathematics, University at Buffalo, The State University of New York. It was presented in an undergraduate research poster fair, UB's Annual Celebration of Student Academic Excellence in April 2017. It was written in the senior Honors thesis submitted to the Department of Mathematics and University Honors College, University at Buffalo in May 2017.

The simple version of application for Chapter 4 was completed by the student, under the supervision of Dr. Yunlong Zhang, the committee chair. It was submitted as the term paper for CVEN 617 Traffic Engineering: Characteristics in December 2017.

All other work conducted for the thesis was completed by the student independently.

Funding Sources

There are no outside funding contributions to acknowledge related to the research and compilation of this document.

NOMENCLATURE

AADT	Annual Average Daily Traffic
SMS	Space Mean Speed
TMS	Time Mean Speed
LOS	Level of Service
PW model	Payne-Whitham model
HCM	Highway Capacity Manual
ITS	Intelligent Transportation Systems
ATMS	Advanced Traffic Management System
BPNN	Back Propagation Neural Network
ARIMA	Autoregressive Integrated Moving Average
PDE	Partial Differential Equation
LWR model	Lighthill–Whitham–Richards model
FFS	Free Flow Speed
v/c ratio	volume capacity ratio
MAPE	Mean Absolute Percentage Error
VAPE	Variance Absolute Percentage Error
PPE	Probability of Percentage Error
GPS	Global Positioning System
Caltrans	California Department of Transportation
PeMS	Caltrans Performance Measurement System
VDS	Vehicle Detector Station

HOV	High-Occupancy Vehicle
SR 99/CA-SR 99	California State Route 99
NB	North Bound
SL	Speed Limit
mph	Mile per hour
vpmpl	vehicle per mile per lane
vph	vehicle per hour

TABLE OF CONTENTS

LIST OF FIGURES

Page

LIST OF TABLES

1. INTRODUCTION

This chapter introduces three traffic variables focused in this study, that is, flow, speed and density. Then it briefs the problem statement and why it is important to study.

1.1 Traffic Variables

Flow, speed and density are the fundamental variables to describe macroscopic traffic. There are various counting ways for the number of vehicles in an exposure. For instance, we have 15-min volume, 1-hour flow rate and annual average daily traffic (AADT). Flow usually addresses the number of vehicles per hour. Flow can be counted by humans with traffic counting equipment for small studies, or by loop detectors or other sensors in the field.

Speed describes how fast an object moves. In the context of traffic, two types of speeds are widely studied: space mean speed (SMS) and time mean speed (TMS). The SMS is the average speed of vehicles traveling on a segment of roadway during a specified time; the TMS is the arithmetic average speed of all vehicles passing a spot for a specified time. The TMS is possible to be calculated from spot speeds collected by devices such as a radar speed gun; the SMS is usually calculated with travel times, and can be estimated by TMS or approximated from the speed reported by dual-loop detectors.

Lastly, density presents the compactness of vehicles in an exposure. Density is hard to measure directly by human or detectors. It is usually estimated by occupancy recorded in detector or a basic flow-speed-density relation. We use the flow-speed-density relation to estimate density. A detailed explanation of such relation is provided in section 3.1. Although it is difficult to measure, the value of density plays an important role in traffic evaluations on freeway. For example, the level of service (LOS) on freeway is based on density.

1.2 Problem Statement

Freeway traffic in a near term can vary because of demand changes, existing events (i.e. crashes, lane closures), special geometrics (i.e. weaving areas, bottleneck sections), and associated shockwaves. These variations of traffic cause difficulties in predictions of traffic flow. It is because the variations of traffic depend on how drivers respond to these traffic changes. Hence, it is important to understand and model driver behavior. Driver behavior modelling is categorized into aggressiveness, familiarity, cooperation and anticipation. In this research, we study a macroscopic traffic model, Payne-Whitham (PW) model, with an anticipation source term. The anticipation source describes how the traffic adjusts its speed based on the condition ahead. For an instance, the speed of traffic flow decreases when the driver notices congestion ahead. The anticipation parameter of the source term is calibrated through this study.

With the calibration of driver's anticipation effect in PW model, this study 1) proposes a short-term freeway traffic prediction method, 2) validates the method with real world traffic data sets3) assess the method by statistical tests, 4) compare the method in different traffic conditions and prediction periods. The traffic prediction method developed in this study differs from data-driven prediction methods. It is derived from the solutions of PW models; hence, it underlies flow studies and the process includes the concept of traffic dynamics.

2. BACKGROUND

Short-term prediction of traffic variables, such as speed, density, and flow, is a trending research topic. With the rise of Intelligent Transportation Systems (ITS), short-term prediction becomes essential in control and management systems, such as Advanced Traffic Management System (ATMS). An accurate short-term prediction benefits the traffic control of both freeway and urban network under congested conditions. Previous literature and studies involve forecast or prediction of traffic through different methods. According to a study conducted by Van Lint [1] in 2007, the most common prediction models are back propagation neural network (BPNN) [2, 3], k-Nearest Neighbor [4], and Autoregressive Integrated Moving Average(ARIMA) [5-7]. Most of these prediction studies are based on data analysis (data-driven), i.e., the prediction method itself does not considers the theories and principles of traffic. The prediction method in this study will be developed from analytical solutions of a macroscopic traffic flow model, Payne-Whitham (PW) model. It is a famous 2nd order dynamic traffic model, introduced in the 1970s by Payne [8] and Whitham [9]. In particular, we consider the effect of driver's behavior by calibrating the anticipation parameter in the PW model. Anticipation behavior can be seen as the driver’s awareness of conditions ahead, and it produces a diffusion, or smoothing of the basic traffic flow wave.

The study will propose a prediction method for the speed and density in a short-term period considering driver’s anticipation effect. This method will be validated through real-world traffic data sets under various durations and different level of congestions. The strength and weakness of the method will also be addressed.

3. METHODOLOGY

This chapter begins with a detailed introduction of Payne-Whitham Model (PW Model) in section 3.1. It discusses and explains the model in terms of its physical meanings and implementations in traffic. Then, a reduced PW Model along with the driver's anticipation source term is formulated and converted into a homogeneous partial differential equation (PDE) system. This system is further decoupled by characteristic variables and solved analytically in section 3.2. The analytical solutions of speed and density are presented by characteristic variables, thus, in section 3.3, they are interpreted by the methods of perturbation and interpolation. Lastly, in section 3.4, some common statistical forecasting performance tests are introduced to evaluate the performances of our predictors.

3.1 Payne-Whitham Model

Speed (i.e. space mean), density and flow (also known as service flow rate or volume) are three significant traffic variables when considering traffic predictions and managements. These three hold a fundamental relation,

$$q = v\rho \tag{1}$$

where, q is the flow, v is the space mean speed and ρ is the density. There are many traffic models describing the traffic from difference scopes. The PW model is a macroscopic traffic model for space mean speed v and density ρ at location x and time t, includes both conservation equation and momentum equation as below,

$$\rho_t + (\rho v)_x = 0 \tag{2}$$

$$v_t + v v_x = \frac{V(\rho) - v}{\tau} - \frac{A(\rho)_x}{\rho} + \mu \frac{v_{xx}}{\rho}. \tag{3}$$

It was developed by H.J. Payne [8] and G.B. Whitham [9] in 1970s independently. The conservation equation, Equation (2), is from the Lighthill and Whitham [10] and Richards [11], or the LWR model. It is a scalar PDE. The conservation equation itself describes the traffic is in an equilibrium state, that is, the input of the traffic is equal to the output. It assumes the speed depends on density, meaning density is a function of speed, which sometime is not true in the reality. For instance, the speed of traffic under same density may slow down because of relative drivers' reactions. The momentum equation of the PW model, Equation (3), links speed and density, so that the speed and density can be independent.

The momentum equation is derived from the Navier-Stokes equation of motion for a 1-D compressible flow, but the source terms are modified. The first source term is the relaxation term, $\frac{V(\rho)-v}{\tau}$; it describes the process in which the driver adjusts the vehicle speed to return the equilibrium traffic speed $V(\rho)$ (i.e. speed limit). The second source term is the anticipation term, $-\frac{A(\rho)_x}{\rho}$; it adjusts the model by reducing the traffic flow when there is a traffic pressure ahead. The last source term is the viscosity term, $\mu \frac{v_{xx}}{\rho}$; it gives a more realistic constitutive relationship between the average reaction time of drivers and the car density.

Note that the anticipation source term describes how the traffic adjusts its speed based on the condition ahead. For instance, the speed of traffic flow decreases when the driver notices congestion ahead. Anticipation behavior can be seen as the driver's awareness of conditions ahead, and it produces a diffusion, or smoothing of the basic traffic flow wave. In the study of

PW model by Kachroo [12], the following expression for anticipation $A(\rho)$ fitted the traffic wave well,

$$A(\rho) = \beta^2 \rho. \tag{4}$$

Here, β is the anticipation rate (units length/time). In traffic flow, the rate is a positive value, as Whitham argues that drivers decrease their speed to account for an increasing density ahead. If we insert Equation (4) into (3), the full PW model is also equivalent to,

$$\rho_t + (\rho v)_x = 0 \tag{5}$$

$$(\rho v)_t + (\rho v^2 + \beta^2 \rho)_x = \frac{V(\rho) - v}{\tau} + \mu \frac{v_{xx}}{\rho}. \tag{6}$$

For this study, we assume the relaxation term and viscosity term are negligible, and focus on a reduced PW model with driver's anticipation effect as,

$$\rho_t + (\rho v)_x = 0 \tag{7}$$

$$(\rho v)_t + (\rho v^2 + \beta^2 \rho)_x = 0. \tag{8}$$

Although Daganzo [13] claimed the PW model and other 2nd order models are straightly following the isotropic fluid dynamics, which is against the anisotropic nature of traffic, as it is one of the earlier developed second-order continuum traffic model with considerations on driver's behavior, PW is indeed the best known and it is worth to be investigated.

3.2 Analytical Solution of PW Model

Previously in section 3.1, we introduced the PW model and reduced it into a system of PDE shown in Equation (7) and (8). It is equivalent to its quasilinear vector form,

$$\boldsymbol{u_t} + \boldsymbol{f}(\boldsymbol{u})\boldsymbol{u_x} = \boldsymbol{0} \tag{9}$$

where,

$$\boldsymbol{u} = \begin{pmatrix} \rho \\ v \end{pmatrix}, \boldsymbol{f}(\boldsymbol{u}) = \begin{pmatrix} 0 & 1 \\ \beta^2 - v^2 & 2v \end{pmatrix}, \boldsymbol{u_x} = \begin{pmatrix} \rho_x \\ (\rho v)_x \end{pmatrix}. \tag{10}$$

In order to obtain implicit solutions through characteristic variables, the system of PDEs in Equation (9), needs to be transferred into two decoupled scalar PDEs. A process of diagonalization is taken place for $\boldsymbol{f}(\boldsymbol{u})$ by assigning $\boldsymbol{A} = \boldsymbol{f}(\boldsymbol{u})$ and diagonalizing $\boldsymbol{A}$ with $\boldsymbol{P}^{-1}\boldsymbol{AP} = \boldsymbol{\Gamma}$. Here, $\boldsymbol{\Gamma}$ is the diagonal matrix with eigenvalues as its diagonals, $\boldsymbol{P}$ is a matrix composed of the eigenvectors of $\boldsymbol{A}$, and $\boldsymbol{P}^{-1}$ is the matrix inverse of $\boldsymbol{P}$. Then, the scalar system of decoupled PDEs is,

$$\boldsymbol{R_t} + \boldsymbol{\Gamma}\boldsymbol{R_x} = \boldsymbol{0} \tag{11}$$

where,

$$\boldsymbol{R_i} \equiv \boldsymbol{P}^{-1}\boldsymbol{u_i} = \begin{pmatrix} \frac{\rho}{2\beta}\left(v + \beta(ln\rho)\right)_i \\ -\frac{\rho}{2\beta}\left(v - \beta(ln\rho)\right)_i \end{pmatrix}, i \equiv x, t; \boldsymbol{\Gamma} = \begin{pmatrix} v + \beta & 0 \\ 0 & v - \beta \end{pmatrix}. \tag{12}$$

Kachroo [12] has solved this scalar PDEs implicitly using the method of characteristics. Let $\boldsymbol{R} = (r_1, r_2)$, the implicit solutions of v, ρ for the reduced PW model with the driver's anticipation parameter is obtained as,

$$\begin{pmatrix} v \\ \rho \end{pmatrix} = \begin{pmatrix} \frac{1}{2}(r_1 + r_2) \\ \exp(\frac{r_1 - r_2}{2\beta}) \end{pmatrix}. \tag{13}$$

3.3 Proposed Prediction Method

Although implicit solutions of v and ρ in Equation (13) are enough to provide an idea of the characteristic solution curve, they are still vague and cannot be applied as they are in terms of characteristic variables. Hence, in subsection 3.3.1, by introducing the perturbation method, explicit solutions are derived. The explicit solution of speed/density is taken as the proposed prediction method of speed/density. The prediction method is then further interpreted through a method of interpolation in subsection 3.3.2. In subsection 3.3.3, a calibration formula for the driver's anticipation parameter is derived and it calibrates the parameter at each time step for the prediction. Lastly, subsection 3.3.4 discusses the benefits and limitations of the prediction methods.

3.3.1 Interpretation of Solution

The perturbation method (aka small disturbance method) is a common mathematical technique to linearize a system of PDEs by the assumption of a steady state with small perturbations departing from itself. The perturbation method is a branch in the family of perturbation expansion solutions to the wave study. The first famous discussion of the method was by Rayleigh [14] in the 1896, the it was further addressed in the work by Rice [15] and Mitzner [16] in the mid-1960s. Recall, we introduced two independent variables (i.e. speed and density) in the PW model, and we assume disturbances $v'(x,t)$ and $\rho'(x,t)$ occurs around their steady states $\bar{v}(x)$ and $\bar{\rho}(x)$, as well as the characteristic variables r_1 and r_2,

$$v(x,t) = \bar{v}(x) + v'(x,t), \qquad \rho(x,t) = \bar{\rho}(x) + \rho'(x,t), \tag{14}$$

$$r_1(x,t) = \overline{r_1}(x) + r_1'(x,t), \qquad r_2(x,t) = \overline{r_2}(x) + r_2'(x,t). \tag{15}$$

Substituting Equation (15) into the scalar system in Equation (11), $\boldsymbol{R_t} + \boldsymbol{\Gamma R_x} = \boldsymbol{0}$, and linearizing for r_1', r_2' gives

$$\frac{\partial r_1'}{\partial t} + (\bar{v} + \beta)\frac{\partial r_1'}{\partial x} = 0, \tag{16}$$

$$\frac{\partial r_2'}{\partial t} + (\bar{v} - \beta)\frac{\partial r_2'}{\partial x} = 0. \tag{17}$$

The Equations (16) and (17) are each one-way wave equation with a constant wave speed. The solution for each is a traveling wave solution in following form,

$$r_1' = f(x - (\bar{v} + \beta)t), \tag{18}$$

$$r_2' = g(x - (\bar{v} - \beta)t). \tag{19}$$

where f, g are arbitrary functions. Let $x_+' := x - (\bar{v} + \beta)t$, $x_-' := x - (\bar{v} + \beta)t$, Equation (18) and (19) can be written in arrow notations,

$$\begin{array}{cc} x \overset{f'}{\rightarrow} x_+' & x \overset{g'}{\rightarrow} x_-' \\ v(x,t) \overset{f'}{\rightarrow} v_f'(x_+',t) & v(x,t) \overset{g'}{\rightarrow} v_g'(x_-',t) \\ \rho(x,t) \overset{f'}{\rightarrow} \rho_f'(x_+',t) & \rho(x,t) \overset{g'}{\rightarrow} \rho_g'(x_-',t) \end{array} \tag{20}$$

where, v_f', v_g', ρ_f' and ρ_g' are the outputs of speeds and densities through the perturbations f', g' of arbitrary functions f, g.

By substituting back into the implicit solutions in Equation (13), the explicit solutions $\hat{v}$ and $\hat{\rho}$ for traffic speed (i.e. space mean speed) and traffic density are derived as,

$$\begin{pmatrix} \hat{v} \\ \hat{\rho} \end{pmatrix} = \begin{pmatrix} \bar{v} + \frac{1}{2}[v_f'(x_+', t) + v_g'(x_-', t)] \\ \bar{\rho}\exp\left(\frac{\rho_f'(x_+', t) - \rho_g'(x_-', t)}{2\beta}\right) \end{pmatrix}. \tag{21}$$

The explicit solutions can be considered as a prediction method for the traffic speed and density, as they take the steady state of speed/density and the solutions of traveling waves as inputs. The steady states can be approximated by taking an arithmetic mean on the historical speeds and densities respectively, while the solutions of traveling waves are relatively difficult to compute. In the next section, we will introduce a method of interpolation to interpret the solutions of traveling.

3.3.2 Method of Interpolation

In the previous section, a prediction method is proposed as a combination of the steady states and the solutions of traveling waves. Consider we have some space and time collections $\{x_i,\ t_j\}_{i=1,\ j=-M}^{i=N,\ j=1}$ along with traffic speed and density $\{v_{ij},\ \rho_{ij}\}_{i=1,\ j=-M}^{i=N,\ j=1}$ or $\{v(x_i, t_j), \rho(x_i, t_j)\}_{i=1,\ j=-M}^{i=N,\ j=1}$. The common examples of such collections are the speed and density from the loop detector stations on freeway. Here, the set $\{v(x_i, t_0), \rho(x_i, t_0)\}_{i=1}^{N}$ is treated as the initial/current data set at initial time t_0, and the set $\{v(x_i, t_1), \rho(x_i, t_1)\}_{i=1}^{N}$ is considered as the data values for future time t_1. The sets $\{v_{ij},\ \rho_{ij}\}_{i=1,\ j=-M}^{i=N,\ j=-1}$ with time $t_{j|j\in\{-W,-W+1,\ldots,-1\}}$ is counted as historical data sets. The index of time has a lower bound, because only those latest historical sets sharing the same steady state with the current sets are counted. Consider these collections are given under a frequency in space with a positive space gap δx, that is $\delta x := x_{i+1} - x_i > 0$ for $\forall i \in \{1,2, \dots, N-1\}$. Such constant space gap is assumed to be consistent over time, since in the real world the locations of loop detectors are fixed over time. These collections are also considered with a frequency in time with a positive time period δt, that is $\delta t := t_j - t_{j-1} > 0$ for $\forall j \in \{0, -1, -2, \dots, -M+1\}$. Notice, such time period is assumed to be a constant among historical data sets. Lastly, the prediction period between initial t_0 and predict time t_1 is defined as Δt, $\Delta t := t_1 - t_0 > 0$. It is not necessary to have Δt equal to δt, but it is bounded on the left by δt, $\delta t \leq \Delta t$, because δt is the smallest period in time.

By applying the prediction method on these data sets, a predicted data set $\{\hat{v}(x_i, t_1), \hat{\rho}(x_i, t_1)\}_{i=1}^{N}$ is expected. Recall in Equation (21), a predicted speed $\hat{v}(x_i, t_1)$ takes $\bar{v}(x_i), v_f'(x_{+i}', t_0)$ and $v_g'(x_{-i}', t_0)$ at each location i as inputs; a predicted density $\hat{\rho}(x_i, t_1)$ takes $\bar{\rho}(x_i), \rho_f'(x_{+i}', t_0)$ and $\rho_g'(x_{-}', t_0)$ at each location i as inputs. Hence, because inputs are computed under the same steps for both speed and density, a generalized variable ϕ will be used, such that $\phi \in \{v, \rho\}$. In the following paragraph, $\bar{\phi}(x_i)$, $\phi_f'(x_{+i}', t_0)$ and $\phi_g'(x_{-i}', t_0)$ will be determined.

The steady state $\bar{\phi}(x_i)$ is obtained by the approximation of the arithmetic mean on the historical and current data sets over time,

$$\bar{\phi}(x_i) = \frac{1}{M+1} \sum_{j=-W}^{j=0} \phi(x_i, t_j) \text{ for } i = 1,2,..,N. \tag{22}$$

The $\phi'_f(x'_{+i}, t_0)$ and $\phi'_g(x'_{-i}, t_0)$ are the outputs of the variable through the perturbations f', g' of arbitrary functions f, g at a location i. That is, the functions are varies at different locations. Thus, it is necessary to compute a general mapping. If a solution of the traveling traffic wave is known, then an exact mapping can be derived. However, the solutions of the traffic wave are unknown. Hence, a method of interpolation is implemented to obtain $\phi'_f(x'_{+i}, t_0)$ and $\phi'_g(x'_{-i}, t_0)$ at a location i. Interpolation is a method in the field of numerical analysis. It estimates unknown values of data points using points with known values. A summary of interpolation is shown in Figure 1 below.

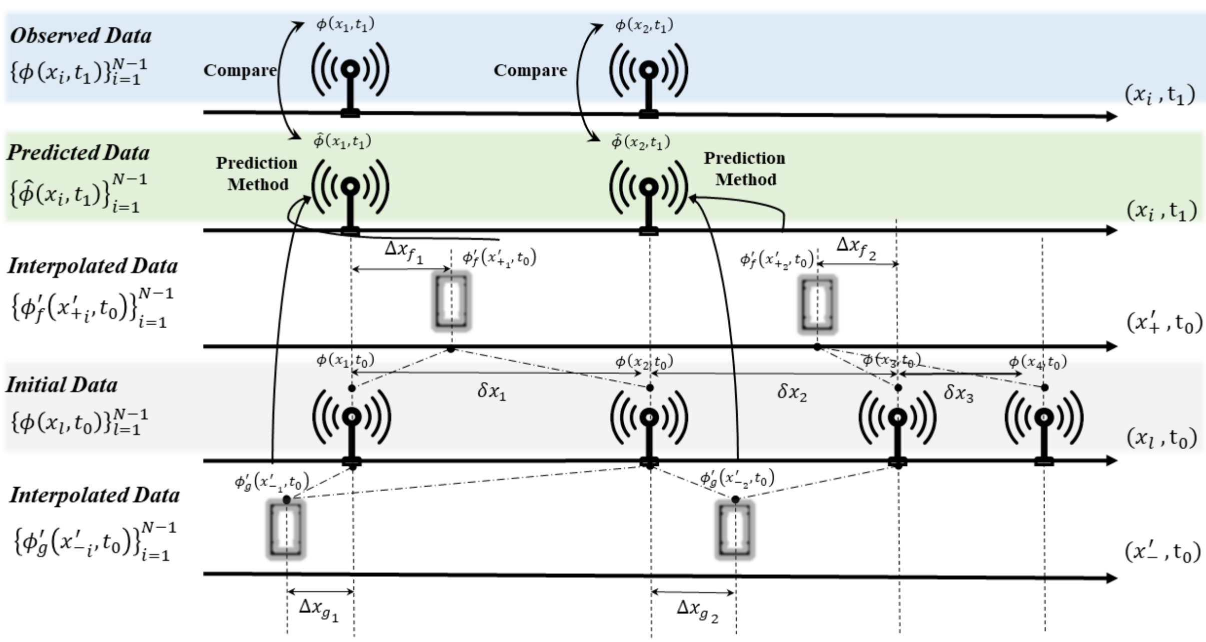

Figure 1 Method of Interpolation with Exemplary Data

As illustrated in Figure 1 above, at the interpolation step, for every value of $\phi_f'\left(x'_{+i}, t_0\right)$ at a location $i \in \{1,2, \dots N\}$ is estimated by $\phi(x_{l+1}, t_0)$ and $\phi(x_l, t_0)$ at a location l. The location l with value x_l is chosen by the following criterial for each given x'_{+i} at initial time t_0,

$$\left|x'_{+i} - x_l\right| = \min\left(\left|x'_{+i} - \{x_k\}_{k=1}^{N-1}\right|\right) \text{ for } i = 1,2,..,N. \tag{23}$$

Such absolute difference above is defined as Δx for each x'_{+i}. Apparently, Δx is not necessary to be δx, which δx was defined as the difference between x_{l+1} and x_l in the earlier paragraph. Therefore, $\phi_f'\left(x'_{+i}, t_0\right)$ is approximated by interpolation as,

$$\phi_f'\left(x'_{+i}, t_0\right) \cong \phi\left(x_j, t_0\right) + (\Delta x)_{f_i} \frac{\phi(\, x_{l+1}\,, t_0) - \phi(x_l, t_0)}{(\delta x)_l} \text{ for } i, l = 1,2,..,N-1. \tag{24}$$

Similarly, $\phi_g'\left(x'_{-i}, t_0\right)$ is interpolated as

$$\phi_g'\left(x'_{-i}, t_0\right) \cong \phi(x_i, t_0) + (\Delta x)_{g_i} \frac{\phi(x_{l+1}, t_0) - \phi(x_l, t_0)}{(\delta x)_l} \text{ for } i, l = 1,2,..,N-1. \tag{25}$$

Then, substituting interpolated variables and the approximated steady state to Equation (22), the predicted speed and density at each location i is determined as,

$$\begin{pmatrix} \hat{v}(x_i, t_1) \\ \hat{\rho}(x_i, t_1) \end{pmatrix} = \begin{pmatrix} \bar{v}(x_i) + \frac{1}{2}\left[v_f'\left(x'_{+i}, t_0\right) + v_g'\left(x'_{-i}, t_0\right)\right] \\ \bar{\rho}(x_i) \exp\left(\frac{\rho_f'\left(x'_{+i}, t_0\right) - \rho_g'\left(x'_{-i}, t_0\right)}{2\beta}\right) \end{pmatrix}. \tag{26}$$

As can be seen, Equation (26) is ready to implement except the unknown driver's anticipation parameter β. The calibration process of it is documented in the next section.

3.3.3 Calibration of Driver's Anticipation Effect

Previously in section 3.1, we introduced the anticipation source term $A(\rho)$ in the PW traffic model, along with its parameter β, as Kachroo [12] suggested the relation $A(\rho) = \beta^2\rho$ to describe the anticipation source term. The anticipation source term describes how the traffic adjusts its speed based on the condition ahead. Correspondingly, driver's anticipation parameter quantifies the representative driver's behavior in the current traffic accounting for a density change downstream.

In order to accurately predict the density, the anticipation parameter needs to be calibrated. We will again assume a small perturbed density $\rho'(x,t)$ occurs around its steady state $\bar{\rho}(x)$ and apply the perturbation assumption to the reduced PW model as formulated in Equation (7) and (8). Then a linearized system is found as below,

$$\rho'_t + \rho'_x\bar{v} + \bar{\rho}v'_x = 0, \tag{27}$$

$$v'_t + \bar{v}\, v'_x + \frac{\beta^2\rho'_x}{\bar{\rho}} = 0. \tag{28}$$

Because the Equation (27) and (28) form a linear constant coefficient system, we could assume the solution of such linearized system is as following,

$$\begin{bmatrix}\rho' \\ v'\end{bmatrix} = \begin{bmatrix}\rho_0 \\ v_0\end{bmatrix} e^{iqx+\sigma t}. \tag{29}$$

Inserting Equation (29) to the linear constant coefficient system, we obtain the following,

$$(\sigma + \bar{v}iq)\rho_0 + (iq\bar{\rho})v_0 = 0, \tag{30}$$

$$(\sigma + \bar{v}iq)v_0 + \left(\frac{\beta^2}{\bar{\rho}}iq\right)\rho_0 = 0, \tag{31}$$

which is equivalent to the matrix form,

$$\begin{bmatrix} \sigma + \bar{v}iq & iq\bar{\rho} \\ \frac{\beta^2}{\bar{\rho}}iq & \sigma + \bar{v}iq \end{bmatrix} \begin{bmatrix} \rho_0 \\ v_0 \end{bmatrix} = 0. \tag{32}$$

Nontrivial solutions require the determinant to be zero, which gives a relation for the growth rate σ,

$$(\sigma + \bar{v}iq)^2 - (iq\bar{\rho}) * \frac{\beta^2}{\bar{\rho}}iq = 0 \implies \sigma = -iq(\bar{v} \pm \beta). \tag{33}$$

Then, disturbances of v, ρ are solved as,

$$\begin{bmatrix} \rho' \\ v' \end{bmatrix} = \begin{bmatrix} \rho_0 \\ v_0 \end{bmatrix} e^{iq(x-(\bar{v}\pm\beta)t)}. \tag{34}$$

We observe that since σ is purely imaginary as shown in Equation (34), the disturbance is not unstable but corresponds to a traveling waves with speed $\bar{v} \pm \beta$. The speed of traveling wave c and steady state of speed $\bar{v}$ are implemented to calibrate anticipation parameter as,

$$\beta = \sqrt{(\bar{v} - c)^2}, \tag{35}$$

where, the speed of travelling wave $c(\rho) = (v(\rho) + v'(\rho)\rho)$ can be derived from the conservation equation, Equation (2).In traffic flow, the rate is assumed to be a positive value, as Whitham [9] argues that drivers decrease their speed to account for an increasing density ahead.

Likewise, we consider data collections $\{v(x_i, t_j), \rho(x_i, t_j)\}_{i=1,\ j=-M}^{i=N,\ j=1}$ along some freeway segments and time durations. Assume a linear relation between $v(\rho)$ and ρ, we fit $v(\rho)$ with $m_i * \rho(x_i, t_j) + b_i$ at each location i with a slope m_i and an intercept b_i. This gives the derivate of $v(\rho)$ to be m_i at each location i,

$$\beta = \sqrt{\left(\frac{1}{W+1}(\sum_{j=-M}^{j=0} v(x_i, t_j)) - v(x_i, t_j) - m_i\, \rho(x_i, t_j)\right)^2}. \tag{36}$$

3.3.4 Limitations

Recall, in order to interpret the implicit solutions of the PW model, a perturbation method was assumed. It assumes the traffic variable owns a small disturbance from its steady state. From a traffic operation point of view, this indicates that the traffic is within the same traffic state during the prediction period. The traditional way to classify traffic state on freeway is the level of service (LOS). LOS is a quantitative stratification of a traffic measurement that indicates the quality of service. The methods to define LOSs are different based on facility types. For instance, different criteria apply to waving segments than basic freeway segments. The standard of LOSs and their detailed calculations are documented in Highway Capacity Manual (HCM) 2010 [17]. Table 1 shows the threshold for each LOS (i.e. traffic state) on different traffic variables at each criterion listed in HCM 2010 [17] for a basic freeway segment with a 70 mph free flow speed

(FFS). The criteria comprise traffic density, along with traffic speed, volume-capacity ratio (aka v/c ratio) and service flow rate (commonly known as hourly volume).

Table 1 LOS Criteria for Basic Freeway Segments

Criteria (FFS = 70mph)	LOS				
	A	B	C	D	E
Density (vpmpl)	< 11	$(11, 18]$	$(18, 26]$	$(26, 35]$	$(35, 45]$
Speed (mph)	> 70	> 70	> 68.2	> 61.5	> 53.3
v/c ratio	< 0.32	< 0.53	< 0.74	< 0.90	< 1.00
Service flow rate (vph)	< 770	< 1260	< 1770	2150	> 2400

From the criteria for a basic freeway segment with a FFS at 70 mph, the range of speed $R_{v_{A\ to\ E}}$, varies from LOS A to F is about 17 mph; the maximum range for speed, max R_v, within a LOS is about 10 mph. The range of speed limits the absolute different in speed (i.e. v_f, v_g) as,

$$|v_f - v_g| < R_{v_{A\ to\ E}}, \tag{37}$$

And, the maximum range for speed within a LOS limits the perturbed speeds (i.e. v_f', v_g') and the combination of perturbed speeds as,

$$\left|v_f' + v_g'\right| < 2 * (\max R_v)\ . \tag{38}$$

Likewise, the range of density $R_{\rho_{A\ to\ E}}$, varies from LOS A to F is about 34 $pcpmpl$; the maximum range for density, max ρ, within a LOS is about 10 $pcpmpl$. The range of density limits the absolute different in density (i.e. ρ_f, ρ_g) as,

$$|\rho_f - \rho_g| < R_{\rho_{A\ to\ E}}, \tag{39}$$

And, the maximum range for density within a LOS limits the perturbed densities (i.e. ρ'_f, ρ'_g) and the combination of perturbed speeds as,

$$|\rho'_f - \rho'_g| < R_\rho. \tag{40}$$

3.4 Statistical Performance Tests

As we interpreted the PW solutions into predictors of space mean speed v, density ρ and flow q(indirectly using the general relation between flow density and speed), the following statistical errors and performance tests are introduced in this section to evaluate the goodness of these predictors:

- Mean absolute percentage error (MAPE)
- Variance absolute percentage error (VAPE)
- Probability of percentage error (PPE)

They are common performance tests to evaluate predictions and forecasts.

The mean absolute percentage error (MAPE) is a statistical measure for the prediction accuracy of a forecasting method. The MAPE is implemented as a primary performance test by Xie [18] to evaluate the volume forecasting models using Kalman Filter with discrete wavelet decomposition. The MAPE calculates the average relative error between the predicted value and actual observed value as,

$$MAPE\ (\%) = 100\% * \frac{1}{N}\sum_{k=1}^{N}\left|\frac{\hat{\phi}_k - \phi_k}{\phi_k}\right|. \tag{41}$$

where, ϕ represents a generalized variable, that is, it can be v, ρ and q; $\hat{\phi}$ indicates the corresponding predicted variable.

The variance of absolute percentage error (VAPE) is the sum of the deviations from the average performance in the forecasting period, as formulated below,

$$VAPE(\%) = \sqrt{\frac{N \sum_{k=1}^{N} \left|\frac{\hat{\phi}_k - \phi_k}{\phi_k}\right|^2 - \left[\sum_{k=1}^{N} \left|\frac{\hat{\phi}_k - \phi_k}{\phi_k}\right|\right]^2}{N(N-1)}}. \tag{42}$$

By definition, a small VAPE indicates the predictor is more stable than those with larger VAPE values. Zheng [19] listed VAPE along with MAPE as the performance test, when Zheng compared the flow prediction with the back propagation neural network, the radial basis function neural network and Bayesian combined neural network model.

Lastly, we assess the predicted values using the probability of percentage error (PPE) by analyzing the percent cases with error greater than $e\%, e \geq 0$. PPE is formatted as,

$$PPE\ (\%) = P\left(\left|\frac{\hat{\phi}_k - \phi_k}{\phi_k}\right| > e\right). \tag{43}$$

It can further separate into underestimated PPE_U and overestimated PPE_O percent cases as,

$$PPE_U\ (\%) = P\left(\frac{\hat{\phi}_k - \phi_k}{\phi_k} < -e\right) \tag{44}$$

$$PPE_O\ (\%) = P\left(\frac{\hat{\phi}_k - \phi_k}{\phi_k} > e\right) \tag{45}$$

Williams [20] applied the PPE as the primary evaluator when analyzing missing values and outliers for urban freeway traffic flow predictions.

These three performance measures (i.e. MAPE, VAPE, PPE) will be used in Chapter 5 for the comparisons and discussion of results.

4. APPLICATION

In this chapter, we first introduce the data source in section 4.1 and the data collection site and date in section 4.2. Then, we take one example data set to perform the PW prediction method in section 4.3 and assess the method using five tests and 4.4.

4.1 Data Source

In order to find the right data source, we first identify the criteria required by PW method:

- Freeway traffic data - PW model is designed to predict highway traffic.
- Well distributed detectors with GPS position – It is to ensure there are significant enough amount of data. The GPS position is needed for interpolation.
- Performance measurements (i.e. flow, speed) recorded in each VDS
- Small data collection period – Short term predictions are typically with a prediction period less than 1-hour.

There are various traffic data platforms provided by cities or states, such as TranStar in Houston, Caltrans PeMS in California, WisTransPortal in Wisconsin. PeMS is the most well-established open source data for freeway performance among those. PeMS was first developed as a freeway analysis tool, and now it is a centralized traffic data warehouse with real-time and historical data from nearly 40,000 individual detectors over the freeway system across all major metropolitan areas of the State of California. A detector measures the number of vehicles (flow or volume) passing, how long they remain over the detector (occupancy) and how fast vehicle passing through two consecutive detectors (speed). The detector reports data on a cycle of 30-second to the controller (i.e. loop detector station), and PeMS aggregate them into a minimal of

5-min performance measurements. In this study, we use the measurements from vehicle detector station (VSD). Those measurements are aggregated data over a set of detectors covering all lanes in one direction of travel at one point (or small segment). VSD monitors facilities like on-ramp, off-ramp, mainline and high-occupancy lane (HOV). For this study, we only consider the VSD on the mainline with its position (i.e. absolute postmile) and 5-min aggregated measurements (i.e. speed and flow).

4.2 Data Collection Site and Time

We choose the northbound direction on California State Route 99 (CA-SR 99 NB) as the data collection site in this study. It is a 6-lane highway about 380-mile long with a speed limit of 70 mph. The northbound starts from Interstate 5 near Wheeler Ridge to California State Route 36 near Red Bluff. It connects cities including Bakersfield, Delano, Tulare, Visalia, Kingsburg, Selma, Fresno, Madera, Merced, Turlock, Modesto, Stockton, Sacramento, Yuba City and Chico. There is a total of 308 VSDs on the mainline of CA-SR 99 NB with 60% of the VSDs aggregated through 3 lanes, 33% aggregated through 2 lanes and 7% aggregated through 4 lanes. Among these VSDs, 95% of the stations is away from their upstream station no longer than 3-mile. A lane configuration diagram generated by PeMS. Figure 2 shows how the mainline VDSs link on a highway segment.

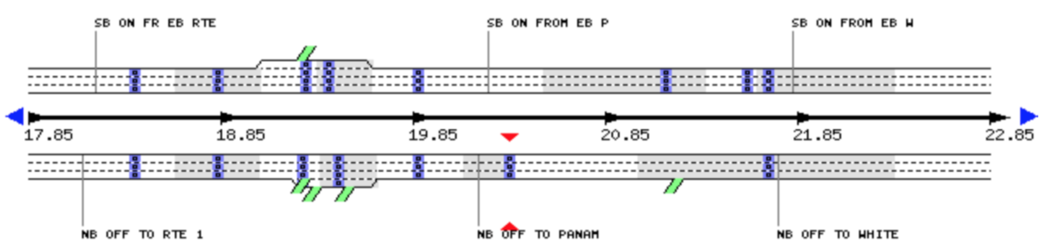

Figure 2 Lane Configuration Diagram for CA-SR 99 NB (Generated by PeMS)

The data collection date is Wednesday, January 16th, 2018. It is an ordinary weekday with a 62% observation rate from detectors. It is with a clearly identified AM Peak from 8:00 AM to 9:00 AM with around 25% of vehicles experiencing a LOS D or worst; PM Peak from 4:00 PM to 5:00 PM with around 10% of vehicles experiencing a LOS D or worst in the time series contour of LOS, Figure 3. Figure 3 illustrates AM Peak lasted longer and heavier than PM Peak. Since it shows the Off-Peak period is from midnight to 4:00 AM at that day with almost 100% of vehicle experiencing a LOS A, we choose the Off-Peak period as from 2:00 AM to 3:00 AM.

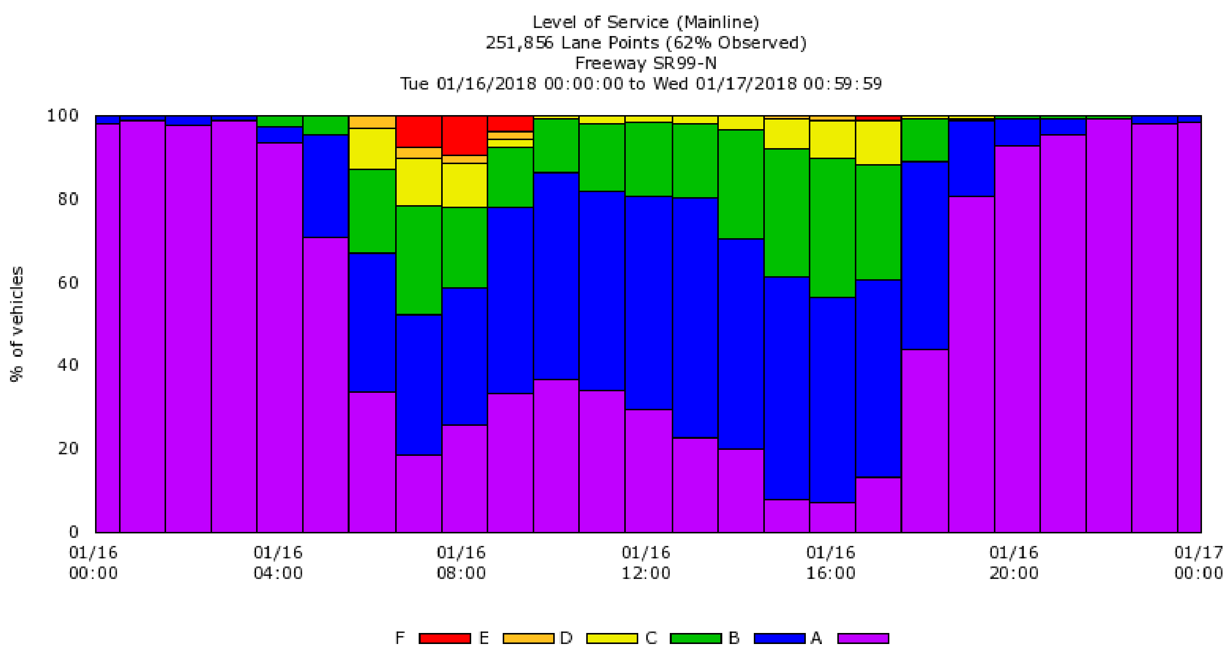

Figure 3 Time Series Contour for Level for Service (Generated by PeMS)

To better understand the collection periods, we generate a speed profile along with bottlenecks in PeMS. PeMS identifies a bottleneck if travel speed is lower than 60 mph. As plotted in Figure 4, the major bottleneck locates at the 300-postmile. It is near the city of

Sacramento, the capital city of California. It is certainly one of the busiest cities on CA-SR 99, and reasonable to see bottlenecks there.

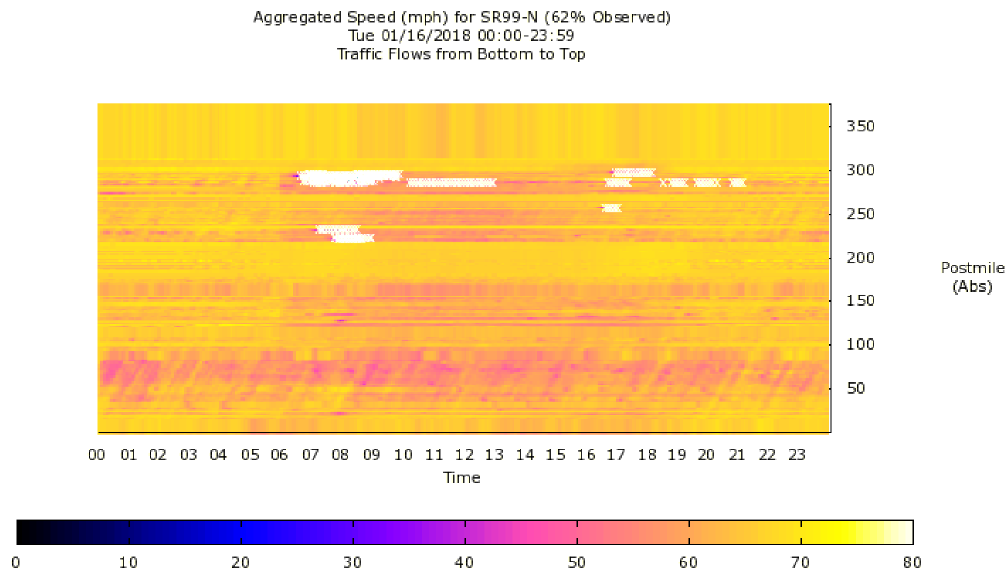

Figure 4 Time Series Contour for 5-minute Speed (mph) (Generated by PeMS)

4.3 Statistical Data Description

As addressed in previous section, we collect speed and flow for AM Peak, PM Peak and Off-Peak periods along CA-SR 99 NB on January 16, 2018. The prediction based on each period are identical. In section 4.3 and 4.4, we illustrate the process using AM Peak as an example.

Before performing predictions, we first summarize the 5-min aggregated speed measurements in Table 2. During the AM Peak, the mean speed for each 5-min interval across CA-SR 99 NB is about 60 mph. The standard deviations are about 11 mph, but with a largest difference in speed about 57 mph. This tells that there are a small portion of VDSs located at the bottlenecks with outputs varying extremely from others. It agrees with the general observation in the previous section.

Table 2 Summary Statistics of 5-min Aggregated Speed (SL 70 mph)

Speed (mph), CA-SR 99 NB, AM Peak, January 16, 2018, 308 VDSs					
Initial Time	Min	Max	Range	Mean	Standard Deviation
8:00 AM	5.80	72.10	66.30	59.41	12.37
8:05 AM	7.40	70.70	63.30	59.24	12.10
8:10 AM	11.60	71.10	59.50	59.10	11.84
8:15 AM	10.50	69.80	59.30	59.03	11.61
8:20 AM	13.50	70.00	56.50	58.96	11.77
8:25 AM	12.90	68.90	56.00	58.87	11.53
8:30 AM	11.00	69.70	58.70	58.92	11.16
8:35 AM	10.30	70.50	60.20	59.37	10.65
8:40 AM	15.70	69.40	53.70	59.27	10.69
8:45 AM	18.00	69.50	51.50	59.25	10.50
8:50 AM	16.40	69.10	52.70	59.39	10.40
8:55 AM	13.50	69.30	55.80	59.57	9.79

Flow is another measurement that can be directly outputted from PeMS. Then we calculate density based on flow and speed. A statistical analysis for 5-min aggregated density is summarized in Table 3. During the AM Peak, the mean density for each 5-min interval across CA-SR 99 NB is about 17 vpmpl. This is at the cut-off edge between LOS of B and C. This agree with the time series contour of LOS in the previous section. The standard deviations are about 13 vpmpl, but with a largest difference about 86 vpmpl. This again tells that there are a small portion of VDSs located at the bottlenecks, experiencing extreme congestion than the rest.

Table 3 Summary Statistics of 5-min Aggregated Density (SL 70 mph)

Density (vpmpl), CA-SR 99 NB, AM Peak, January 16, 2018, 308 VDSs					
Initial Time	Min	Max	Range	Mean	Standard Deviation
8:00 AM	0.00	115.17	115.17	18.06	16.83
8:05 AM	0.00	120.00	120.00	17.79	15.86
8:10 AM	1.24	97.09	95.86	17.59	14.05
8:15 AM	0.00	79.43	79.43	17.56	13.64

Table 3 Continued

Initial Time	Min	Max	Range	Mean	Standard Deviation
8:20 AM	0.00	91.56	91.56	17.32	13.54
8:25 AM	0.00	78.55	78.55	17.53	13.80
8:30 AM	0.00	81.01	81.01	16.85	13.12
8:35 AM	0.00	85.05	85.05	16.62	12.73
8:40 AM	2.27	74.90	72.63	16.40	11.90
8:45 AM	0.00	80.89	80.89	16.00	12.22
8:50 AM	0.70	69.36	68.66	15.58	11.52
8:55 AM	0.00	71.55	71.55	14.96	10.83

4.4 Short-term Prediction Results

After reviewing the 5-min aggregated speeds and densities, we perform predictions for AM Peak traffic. In this study, we perform short-term predictions, that is, 5-min, 10-min, 15-min, 20-min, 30-min, 45-min and 60-min (1-hour) predictions. The processes for different prediction periods are identical. In this section (section 4.4), we provide the details of 5-min prediction from 8:00 AM as an example.

Recall in section 3.3, we mentioned the limitation of PW method as it reduces predictable sites in the step of interpolation. That is, the number of predictable VDSs decreases by using PW method. For instance, it has 308 VDSs for speed and density on 8:00 AM, but 239 VDSs out of those are predictable in 5-min using PW methods. Some predictions from those VDSs are in Table 4. At each predictable VDS, a drivers' anticipation parameter is estimated using the equation with historical average and the speed of traffic travelling wave, stated in the section 3.3.3. Recall, the drivers' anticipation parameter describes how drivers react to the traffic ahead.

As visually demonstrated in Figure 5, the value of drivers' anticipation parameter is related to the initial density. The drivers' anticipation parameter is small when the downstream traffic is stable (i.e. a small density value); the parameter is large when the downstream traffic is jammed (i.e. a large density value). The averaged anticipation parameter is computed as 12.0537 for this 5-min predictions on speed and density from 8:00 AM.

Table 4 5-min Speed and Density Predictions based on 8:00 AM, CA-SR 99 NB

VDS ID #	Distance (Postmile)	Estimated Anticipation Parameter	Predicted Speed (mph)	Predicted Density (vpmpl)
601376	0.8	3.2909	62.70	4.05
601931	3.5	2.5407	62.20	4.17
…	…	…	…	…
316922	310.7	3.6110	62.52	5.46
316932	313.1	1.6513	70.71	2.53
318509	376.3	6.1408	67.65	11.11

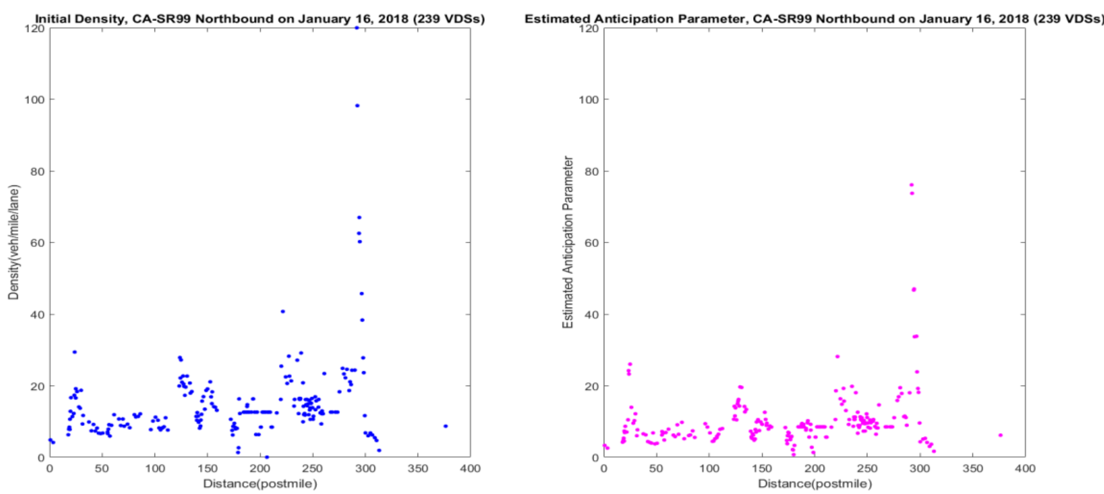

Figure 5 Density and Estimated Anticipation Parameter

Further, we plot 5-min speed predictions (in green) with the initial speed (in black) and observed speed (in blue) in Figure 6. This visually presents that speeds are consistently well-predicted by PW method along the CA-SR 99 NB. Moreover, five statistical performance tests from section 3.4 are applied to assess the 5-min prediction in speed. The results show a 3.47% in MAPE and 5.15% in VAPE for 5-min speed prediction from 8:00 AM. These indicate the average relative error between the predicted speed and actual observed speed in 8:05 AM is 3.47% with a variance of 5.15%. The PPE tests show that only 4.18% of the speed predictions being underestimated, and 5.44% of the speed predictions being overestimated in this example.

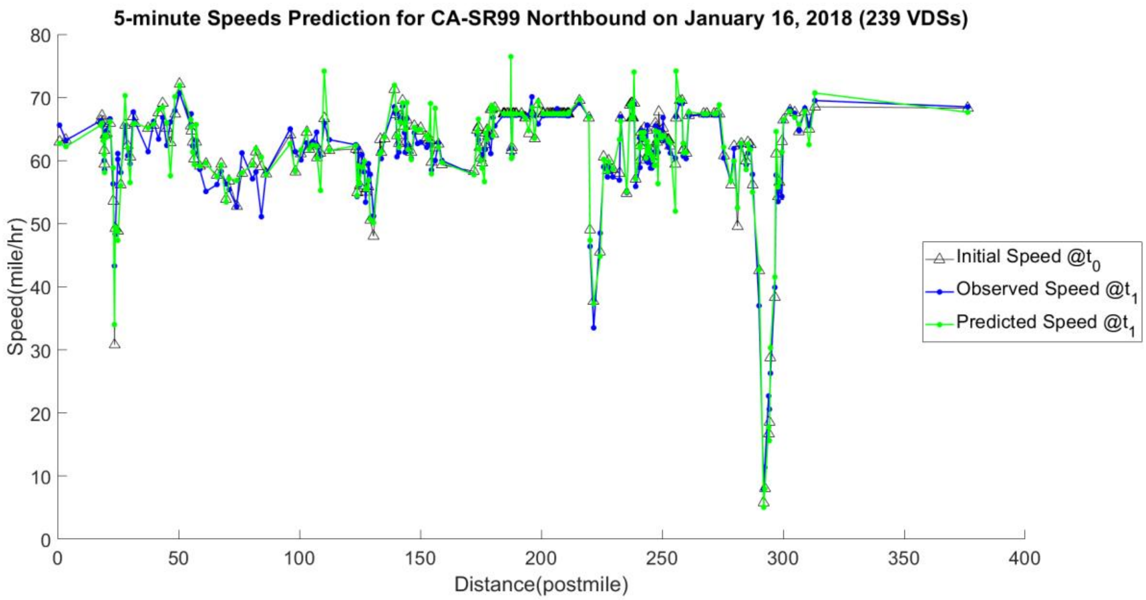

Figure 6 5-minute Speed Predictions

Moreover, we apply the 5-min prediction for all time intervals in AM Peak and assess the speed prediction using five statistical tests. The results are shown in Table 5. We also list the averaged anticipation parameters in Table 5 along with the size of the predictable VDSs.

Table 5 Statistical Performance Tests on 5-minute Speed Predictions

CA-SR 99 NB, AM Peak, January 16, 2018							
Initial Time	Averaged Anticipation Parameter	Number of Predictable VDS	MAPE (%)	VAPE (%)	PPE_U (%)	PPE_O (%)	PPE (%)
8:00 AM	12.0537	239	3.47%	5.15%	4.18%	5.44%	9.62%
8:05 AM	12.1137	233	4.09%	7.63%	3.86%	5.58%	9.44%
8:10 AM	13.1126	233	3.11%	4.86%	3.43%	2.15%	5.58%
8:15 AM	13.0858	238	3.87%	6.42%	4.20%	5.04%	9.24%
8:20 AM	13.1048	235	3.26%	4.12%	2.55%	5.53%	8.09%
8:25 AM	13.0421	243	3.13%	4.75%	2.47%	4.53%	7.00%
8:30 AM	12.5894	235	3.39%	5.19%	3.40%	3.40%	6.81%
8:35 AM	12.0565	250	3.68%	5.86%	4.00%	4.40%	8.40%
8:40 AM	12.8492	244	3.12%	4.22%	2.87%	3.28%	6.15%
8:45 AM	11.9975	249	3.59%	5.79%	3.61%	4.82%	8.43%
8:50 AM	12.1997	250	3.17%	4.39%	4.00%	3.60%	7.60%
8:55 AM	11.6111	248	3.85%	5.56%	4.44%	8.47%	12.90%
Average	**12.4847**	**241**	**3.48%**	**5.33%**	**3.59%**	**4.69%**	**8.27%**

Likewise, we plot 5-min density predictions (in green) with the initial speed (in black) and observed speed (in blue) in Figure 7. Similarly, five statistical performance tests from section 3.4 are applied to assess the 5-min prediction in density by PW method. The results show a 17.51% in MAPE and 19.71% in VAPE for 5-min density prediction from 8:00 AM. This gives a relatively large error comparing with the prediction on speed. One reasonable explanation is the initial density is not a direct output from the VDS. Initial density is computed under the assumption of a fundamental relation between flow and speed.

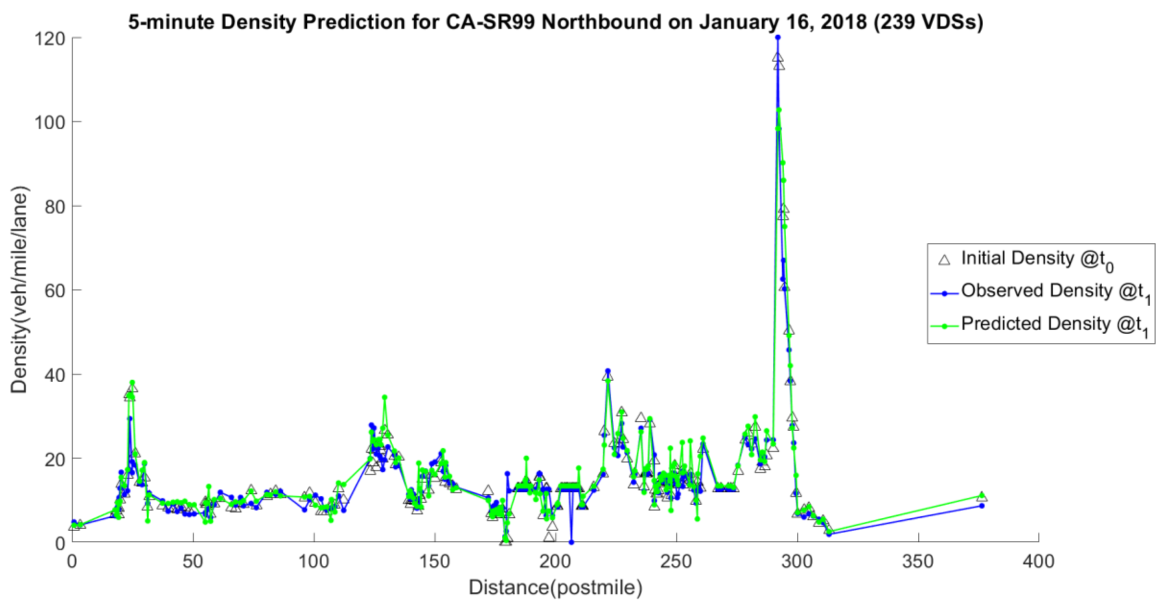

Figure 7 5-minute Density Predictions

Furthermore, we apply the 5-min prediction for all time intervals in AM Peak and assess the speed prediction using the five statistical tests. The results for density predictions are shown in Table 6. We also tabulate the averaged anticipation parameters in Table 6 along with the size of the predictable VDSs.

Table 6 Statistical Performance Tests on 5-minute Density Predictions

CA-SR 99 NB, AM Peak, January 16, 2018							
Initial Time	Averaged Anticipation Parameter	Number of Predictable VDS	MAPE (%)	VAPE (%)	PPE_U (%)	PPE_O (%)	PPE (%)
8:00 AM	12.0537	239	17.51%	19.71%	17.65%	30.67%	48.32%
8:05 AM	12.1137	233	20.46%	49.49%	24.03%	25.32%	49.36%
8:10 AM	13.1126	233	16.50%	42.79%	20.26%	26.72%	46.98%
8:15 AM	13.0858	238	14.46%	23.33%	19.41%	24.05%	43.46%

Table 6 Continued

Initial Time	Averaged Anticipation Parameter	Number of Predictable VDS	MAPE (%)	VAPE (%)	PPE_U (%)	PPE_O (%)	PPE (%)
8:20 AM	13.1048	235	14.35%	17.28%	23.50%	22.22%	45.73%
8:25 AM	13.0421	243	23.52%	76.98%	18.60%	29.75%	48.35%
8:30 AM	12.5894	235	17.71%	84.93%	12.88%	27.04%	39.91%
8:35 AM	12.0565	250	16.60%	23.84%	20.80%	25.60%	46.40%
8:40 AM	12.8492	244	20.02%	83.98%	15.29%	29.34%	44.63%
8:45 AM	11.9975	249	22.89%	120.51%	14.46%	28.11%	42.57%
8:50 AM	12.1997	250	30.40%	175.63%	18.88%	29.32%	48.19%
8:55 AM	11.6111	248	15.96%	20.33%	14.52%	32.26%	46.77%
Average	**12.4847**	**241**	**19.20%**	**61.57%**	**18.36%**	**27.53%**	**45.89%**

4.5 Summary

In this chapter, we introduced PeMS from Caltrans as our data source in section 4.1. Then in section 4.2, we identified the data collection site as CA-SR 99 NB with January 16th, 2018 as collection date and stated the three traffic conditions and seven prediction periods for comparison studies in the next chapter. We took 5-min predictions in AM peak as an example in section 4.3 and 4.4 to perform the PW method and assess the method using five statistical tests. The averaged performance results are summarized in Table 7 below. Because the initial speed is directly output from VDSs, the PW method’s performance in predicting speed is better than density. Thus, we will mainly discuss based on speed prediction in the next chapter.

Although Table 7 demonstrates that speeds are well predicted in 5-min period during AM Peak, we need to further consider whether the traffic conditions and/or length of the prediction periods effect the PW method. We will also discuss more on the drivers’ anticipation parameter in the next chapter to investigate how it is related to the traffic conditions and/or length of the prediction periods.

Table 7 Averaged Performance Results on 5-minute Speed and Density Predictions

CA-SR 99 NB, AM Peak, January 16, 2018							
	Averaged Anticipation Parameter	Number of Predictable VDS	MAPE (%)	VAPE (%)	PPE_U (%)	PPE_O (%)	PPE (%)
Speed	12.4847	241	3.48%	5.33%	3.59%	4.69%	8.27%
Density	12.4847	241	19.20%	61.57%	18.36%	27.53%	45.89%

5. DISCUSSION

In the previous chapter, we show that the PW method is better in predicting speed than density based on 5-min prediction in AM Peak. Then, in this chapter, we investigate more on the drivers' anticipation parameter and the error percentages of speed prediction in different traffic conditions (section 5.1) and different prediction periods (section 5.2). Lastly, in section 5.3, we provide a general recommendation on the anticipation parameter for practitioners to use PW prediction method without knowing the shape of entire traffic travelling wave.

5.1 Comparisons in Different Traffic Conditions

Recall, we identified three traffic conditions on January 16, 2018 for CA-SR 99 NB as AM Peak from 8:00 AM to 9:00 AM, PM Peak from 4:00PM to 5:00 PM, Off Peak from 2:00 AM to 3:00 AM. We first compare the 5-min speed prediction in different traffic conditions.

Table 8 compares the averaged anticipation parameters, numbers of predictable VDS and percentages of error (i.e. MAPE, VAPE, PPE) among AM Peak, PM Peak and Off Peak. It clearly shows that the drivers' anticipation parameter is larger when the traffic is unstable. For example, the AM Peak is experiencing most congestions of a day and the anticipation parameter is with a value of 12.0537. It is about twice larger than the value for the PM peak, and twelve times larger than the one for the Off Peak. On the other hand, Table 8 shows that the number of predictable VDS reduces when the traffic gets more congested. It is because we eliminate a VDS at the step of interpolation if it reports a traffic measurement under a different traffic status (i.e. LOS) from its previous one. The percentages of errors are consistent in Table 8. We can conclude that the ability of PW model is stable in different traffic conditions.

Table 8 Comparisons for Different Traffic Conditions on 5-minute Speed Predictions

CA-SR 99 NB, January 16, 2018							
Traffic Condition*	Averaged Anticipation Parameter	Number of Predictable VDS	MAPE (%)	VAPE (%)	PPE_U (%)	PPE_O (%)	PPE (%)
AM Peak	12.0537	241	3.48%	5.33%	3.59%	4.69%	8.27%
PM Peak	6.1425	265	2.50%	3.42%	1.98%	1.98%	3.96%
Off Peak	1.8119	273	3.51%	4.28%	3.45%	4.68%	8.13%

* AM Peak is the average of 5-min prediction from 8:00 AM to 9:00 AM, PM Peak is from 4:00PM to 5:00 PM, Off Peak is from 2:00 AM to 3:00 AM

Furthermore, we replicate the process and compare 5-min and 10-min speed predictions under different traffic conditions in Table 9. The results for 10-min speed prediction agree with those for 5-min. The percentages of errors do not vary much in different traffic conditions (only slightly worse in general). However, when the traffic gets more congested, the drivers' anticipation parameter turns larger and the size of predictable VDSs gets reduced.

Table 9 Comparisons for Different Traffic Conditions on 10-minute Speed Predictions

Comparisons on 10-minute Speed Predictions, CA-SR 99 NB, January 16, 2018							
Traffic Condition*	Averaged Anticipation Parameter	Number of Predictable VDS	MAPE (%)	VAPE (%)	PPE_U (%)	PPE_O (%)	PPE (%)
AM Peak	12.6516	239	4.33%	6.58%	4.32%	5.93%	10.25%
PM Peak	6.0538	256	3.06%	4.07%	3.31%	3.13%	6.44%
Off Peak	1.8380	266	3.65%	4.35%	4.49%	4.70%	9.19%

* AM Peak is the average of 5-min prediction from 8:00 AM to 9:00 AM, PM Peak is from 4:00PM to 5:00 PM, Off Peak is from 2:00 AM to 3:00 AM

5.2 Comparisons in Different Prediction Periods

In the previous section, we consider comparisons in different traffic conditions for 5-min and 10-min predictions. Further in this section, a detailed comparison in different prediction periods will be addressed. Recall, the possible short-term prediction periods are 5-min, 10-min, 15-min, 20-min, 30-min, 45-min and 60-min based on the same initial speed.

Table 10 Comparisons at AM Peak for Different Prediction Periods

Comparisons on Speed Predictions at AM Peak, CA-SR 99 NB, January 16, 2018							
Prediction Periods (minute)	Averaged Anticipation Parameter	Number of Predictable VDS	MAPE (%)	VAPE (%)	PPEU (%)	PPEO (%)	PPE (%)
5	12.0537	239	3.47%	5.15%	4.18%	5.44%	9.62%
10	12.0537	238	4.55%	7.51%	3.78%	6.30%	10.08%
15	12.0537	233	6.02%	12.47%	6.01%	8.15%	14.16%
20	12.0537	215	7.01%	19.91%	6.98%	8.37%	15.35%
30	12.0537	204	5.33%	5.99%	4.90%	11.76%	16.67%
45	12.0537	210	6.19%	7.13%	6.19%	14.29%	20.48%
60	12.0537	197	6.69%	6.59%	4.06%	19.80%	23.86%

Table 10 tabulates the averaged anticipation parameters, numbers of predictable VDS and percentages of error (i.e. MAPE, VAPE, PPE) among all seven prediction periods for AM Peak. Because prediction periods are all predicting from 8:00 AM, they are with the same drivers' anticipation parameter. Table 10 shows that the number of predictable VDS reduces as the length of prediction period increases. This is because the traffic states have a larger possibility to change when we have a longer prediction period. For example, there are 239 predictable VDSs for a 5-min prediction, but 197 predictable VDSs for a 60-min prediction. It is about 20% reduction. On the other hand, the percentages of errors are relatively small in 5-min and 10-min predictions in Table 10. Thus, we conclude that the ability of PW model is stable in different prediction periods, but we believe that PW model performs more accurately in 5-min and 10-min predictions.

We then replicate the process and combine comparisons in different prediction periods and different traffic conditions in Table 11. When the traffic becomes more stable, the drivers' anticipation parameter turns smaller and the size of predictable VDSs increases. The number of predictable VDS also increases if the length of prediction period is shorter. On the other hand, the percentages of errors do not vary much in different traffic conditions and prediction periods in general. Under the case of congested traffic (i.e. AM Peak), errors are smaller in 5-min and 10-min predictions.

Table 11 Comparisons at all Traffic Conditions for Different Prediction Periods

Speed Predictions in AM Peak*, Initial Time 8:00 AM							
Prediction Periods (minute)	Averaged Anticipation Parameter	Number of Predictable VDS	MAPE (%)	VAPE (%)	PPEU (%)	PPEO (%)	PPE (%)
5	12.0537	239	3.47%	5.15%	4.18%	5.44%	9.62%
10	12.0537	238	4.55%	7.51%	3.78%	6.30%	10.08%
15	12.0537	233	6.02%	12.47%	6.01%	8.15%	14.16%
20	12.0537	215	7.01%	19.91%	6.98%	8.37%	15.35%
30	12.0537	204	5.33%	5.99%	4.90%	11.76%	16.67%
45	12.0537	210	6.19%	7.13%	6.19%	14.29%	20.48%
60	12.0537	197	6.69%	6.59%	4.06%	19.80%	23.86%
Speed Predictions in PM Peak*, Initial Time 4:00 PM							
Prediction Periods (minute)	Averaged Anticipation Parameter	Number of Predictable VDS	MAPE (%)	VAPE (%)	PPEU (%)	PPEO (%)	PPE (%)
5	5.5798	260	2.48%	3.01%	1.92%	1.92%	3.85%
10	5.5798	259	2.98%	3.66%	3.09%zy	3.86%	6.95%
15	5.5798	251	2.81%	3.69%	3.19%	3.19%	6.37%
20	5.5798	252	2.94%	3.36%	1.98%	2.78%	4.76%
30	5.5798	229	3.90%	8.20%	3.06%	4.80%	7.86%
45	5.5798	219	4.03%	13.33%	2.74%	2.28%	5.02%
60	5.5798	196	3.87%	3.86%	6.12%	2.55%	8.67%

Table 11 Continued

Speed Predictions in Off Peak*, Initial Time 2:00 AM							
Prediction Periods	Averaged Anticipation Parameter	Number of Predictable VDS	MAPE (%)	VAPE (%)	PPEU (%)	PPEO (%)	PPE (%)
5	2.3708	280	3.69%	4.09%	3.93%	4.64%	8.57%
10	2.3708	273	3.80%	4.20%	6.23%	4.76%	10.99%
15	2.3708	269	3.53%	3.93%	3.72%	3.72%	7.43%
20	2.3708	260	3.62%	3.74%	2.31%	5.38%	7.69%
30	2.3708	242	3.99%	4.84%	6.20%	3.31%	9.50%
45	2.3708	231	3.72%	3.94%	6.06%	3.03%	9.09%
60	2.3708	215	4.44%	4.81%	6.51%	6.98%	13.49%

*AM Peak is the average of 5-min prediction from 8:00 AM to 9:00 AM, PM Peak is from 4:00PM to 5:00 PM, Off Peak is from 2:00 AM to 3:00 AM

5.3 Driver's Anticipation Effect

As addressed in the problem station (section 1.2), driver's anticipation is essential in traffic modelling and traffic forecasting. It is one branch in driver behavior modelling. It describes how the traffic adjusts its speed based on the condition ahead. For an instance, the speed of traffic flow decreases when the driver notices congestion ahead. An accurate driver's anticipation eliminates the difficulty in traffic predictions through the driver's side.

The calibration of the anticipation parameter in the source term is proposed in section 3.3.3 of the methodology chapter and derived by density and speed data from PeMS in section 4.4 of the application chapter.

The anticipation parameter is further investigated in section 5.1 and 5.2 of this discussion chapter. We compared it through different traffic conditions and different prediction periods. It is found that the drivers' anticipation parameter turns smaller, when the traffic becomes more stable. To validate this observation, we reproduce the calibration process on multiple days. We found the anticipation parameter in LOS A (i.e. Off Peak on CA-SR 99 NB) can be as low as 0, to about 4; it ranges from 3 to 9 during LOS B - LOS C (i.e. PM Peak on CA-SR 99 NB); it varies from 8 to 14 in LOS C - F (i.e. AM Peak on CA-SR 99 NB). These ranges are tabulated in Table 12 for practitioners to refer when they are using the PW traffic model without knowing the shape of traveling wave.

Table 12 Recommendations on Driver's Anticipation Parameter

Statistical Summary of Anticipation Parameter		
Level of Service	Mean	Recommended Range
A	1.8287	0~4
B - C	6.3622	3~9
C - F	11.6458	8~14

6. CONCLUSION

Short-term traffic prediction is critical in advanced traffic management systems (ATMS)and advanced traveler information systems (ATIS). Accurate forecasting results in speed, density or flow are useful to indicate future traffic conditions and assist traffic managers in seeking solutions to congestion problems on freeways. There is a raised research interest in short-term traffic prediction with the developments in intelligent transportation systems (ITS) technologies. Previous research involves data analysis and technologies in many areas, and a significant number of prediction methods exist in the literature. However, most studies used non-parametric predication methods, are data-driven, require data training time/process and have limited forecasting abilities with less data information given. While the PW prediction method developed in this study derived from the solutions of the macroscopic PW traffic flow, it underlies flow studies and the process includes the concept of traffic dynamics.

The proposed PW prediction method validates its ability to predict speed and density in 5-min with PeMS real world data sets from Caltrans. The test results indicate the average relative error between the predicted speed and actual observed speed is 3.48% with a variance of 5.33%. The PPE tests show that only 4.69% of the speed predictions being underestimated, and 8.27% of the speed predictions being overestimated in 5-min speed prediction. The test results in density indicate an average relative error is 19.20%. It is a relatively large error comparing with the prediction on speed. One reasonable explanation is the initial density is not a direct output from the VDS. Initial density is computed under the assumption of a fundamental relation between flow and speed.

Furthermore, we compare the drivers' anticipation parameter and the error percentages of speed prediction in different traffic conditions and different prediction periods. When the traffic becomes more stable, the drivers' anticipation parameter turns smaller and the size of predictable VDSs increases. The number of predictable VDS also increases if the length of prediction period is shorter. On the other hand, the percentages of errors do not vary much in different traffic conditions and prediction periods in general. Under the case of congested traffic (i.e. AM Peak), errors are smaller in 5-min and 10-min predictions.

Lastly, we recommend takes a value between 8 to 14 for the anticipation parameter when modelling the traffic with LOS from C to F. We suggest a range from 3 to 9 for the parameter when modelling the traffic with LOS from B to C. For a traffic with LOS A, the best value for the parameter lies between 0 to 4. These recommendation ranges guide practitioners when using PW model or PW prediction method.

The traffic prediction method developed in this study differs from data-driven prediction methods. It is derived from the solutions of PW model; hence, it underlies flow studies and the process includes the concept of traffic dynamics. It reduces the size of predictable data points, because a perturbation method was assumed in solving the PW model. The results show under a congested traffic, there are about 77.6% of data points satisfied for a 5-min PW prediction, 63.6% of data points satisfied for a one-hour PW prediction. This indicates the limitation does not have large impact on the PW predictions in general.

REFERENCES

1. Van Lint, J. and C. Van Hinsbergen, *Short-term traffic and travel time prediction models.* Artificial Intelligence Applications to Critical Transportation Issues, 2012. 22: p. 22-41.

2. Xie, Y. and Y.J.J.o.I.T.S. Zhang, *A wavelet network model for short-term traffic volume forecasting.* 2006. 10(3): p. 141-150.

3. Huang, S.-H. and B. Ran, *An application of neural network on traffic speed prediction under adverse weather condition*. 2003, University of Wisconsin--Madison.

4. Smith, B.L., B.M. Williams, and R.K.J.T.R.P.C.E.T. Oswald, *Comparison of parametric and nonparametric models for traffic flow forecasting.* 2002. 10(4): p. 303-321.

5. Kamarianakis, Y. and P.J.T.R.R.J.o.t.T.R.B. Prastacos, *Forecasting traffic flow conditions in an urban network: Comparison of multivariate and univariate approaches.* 2003(1857): p. 74-84.

6. Zhang, Y., Y. Zhang, and A. Haghani, *A hybrid short-term traffic flow forecasting method based on spectral analysis and statistical volatility model.* Transportation Research Part C: Emerging Technologies, 2014. 43: p. 65-78.

7. Zhang, Y. and Y. Zhang, *A comparative study of three multivariate short-term freeway traffic flow forecasting methods with missing data.* Journal of Intelligent Transportation Systems, 2016. 20(3): p. 205-218.

8. Payne, H.J., *Models of freeway traffic and control.* Mathematical models of public systems, 1971.

9. Whitham, G. and R.G. Fowler, *Linear and nonlinear waves.* Physics Today, 1975. 28: p. 55.

10. Whitham, G., *On kinematic waves II. A theory of traffic flow on long crowded roads.* Proc. R. Soc. Lond. A, 1955. 229(1178): p. 317-345.

11. Richards, P.I., *Shock waves on the highway.* Operations research, 1956. 4(1): p. 42-51.

12. Kachroo, P. and S. Sastry, *Traffic flow theory–Mathematical framework.* University of California Berkeley, 2006.

13. Daganzo, C.F., *Requiem for second-order fluid approximations of traffic flow*. Transportation Research Part B: Methodological, 1995. 29(4): p. 277-286.

14. Strutt, J.W. and B. Rayleigh, *The theory of sound*. 1945: Dover.

15. Rice, S.O.J.C.o.p. and a. mathematics, *Reflection of electromagnetic waves from slightly rough surfaces.* 1951. 4(2-3): p. 351-378.

16. Mitzner, K.J.J.o.M.P., *Effect of small irregularities on electromagnetic scattering from an interface of arbitrary shape.* 1964. 5(12): p. 1776-1786.

17. National Research Council (U.S.). Transportation Research Board., *Highway capacity manual*. 1 volume (loose-leaf).

18. Xie, Y., Y. Zhang, and Z. Ye, *Short-Term Traffic Volume Forecasting Using Kalman Filter with Discrete Wavelet Decomposition.* Computer-Aided Civil and Infrastructure Engineering, 2007. 22(5): p. 326-334.

19. Zheng, W., D.-H. Lee, and Q.J.J.o.t.e. Shi, *Short-term freeway traffic flow prediction: Bayesian combined neural network approach.* 2006. 132(2): p. 114-121.

20. Williams, B., P. Durvasula, and D.J.T.R.R.J.o.t.T.R.B. Brown, *Urban freeway traffic flow prediction: application of seasonal autoregressive integrated moving average and exponential smoothing models.* 1998(1644): p. 132-141.